Journal of
Applied
Crystallography
ISSN 1600-5767

Received 29 August 2013
Accepted 4 March 2014

Phase-sensitive small-angle neutron scattering

C. F. Majkrzak,[a]* K. Krycka,[a] S. Krueger,[a] N. F. Berk,[a,b] P. Kienzle[a] and B. Maranville[a]

[a]Center for Neutron Scattering, National Institute of Standards and Technology, Gaithersburg, MD 20899, USA, and [b]Department of Materials Science and Engineering, University of Maryland, College Park, MD 20742, USA. Correspondence e-mail: charles.majkrzak@nist.gov

A method is described for determining the neutron scattering length density distribution of a molecular-scale object directly from phase-sensitive small-angle neutron scattering (SANS). The structure factor amplitude is obtained through the use of a reference structure for a collection of randomly oriented, identical objects in the dilute solution limit (negligible interparticle correlations). This work extends some of the techniques developed in recent years for phase-sensitive specular neutron reflectometry to SANS, although the approach presented here is applicable only within the range of validity of the Born approximation. The scattering object is treated as a composite consisting of an 'unknown' part of interest plus a reference component, the real-space structure of the latter being completely known. If, for example, the reference part of the object is composed of a ferromagnetic material (the magnetization of which is saturated), then polarized neutron beams can be employed to extract the information required for an unambiguous inversion of the scattering data without chemical substitution. The angular averaging over all possible relative orientations of the composite object does not result in a cancellation of the phase information since the reference and unknown parts of each object have a fixed spatial relationship. The new approach proposed here is not simply another type of isomorphic substitution, but also involves a reformulation of the underlying mathematical analysis of this particular scattering problem.

1. Introduction

It is well known that the loss of phase information in diffraction studies of condensed matter, whether in crystallography, reflectometry or small-angle neutron scattering (SANS), may lead to ambiguous results for the structure of the scattering object. Mathematical solutions to this problem in the case of X-ray diffraction from crystals were developed by Hauptmann and Karle (Hauptman, 1986) by taking advantage of physical constraints such as that imposed by the positivity of the electron charge distribution within a unit cell of the material. Isomorphic substitution methods have been applied in crystallography, where multiple diffraction data sets are obtained for samples having the same lattice structure but with known substitutions of various atomic species at different sites within the unit cell (Cowley, 1981). Molecular-scale holography (Sur *et al.*, 2001) has also been explored as a method for determining the structures of molecular materials that do not necessarily possess a high degree of translational order between individual molecular units but are well ordered orientationally. Methods involving reference structures have been applied in specular neutron reflectometry to obtain the complex reflection amplitude for an unknown segment of a thin-film structure exactly, thereby enabling a direct first-principles inversion to obtain the scattering length density (SLD) depth profile along the normal to the surface of the film unambiguously (at least to the extent allowed by the finite range over which the reflectivity is measured and the statistical uncertainty in the data) (Majkrzak *et al.*, 1992, 2003; Majkrzak & Berk, 1995; De Haan *et al.*, 1995; Berk & Majkrzak, 1996; Kasper *et al.*, 1998). Phase-sensitive X-ray reflectometry techniques have been developed as well (Lesslauer & Blasie, 1971; Sanyal *et al.*, 1993; Zimmermann *et al.*, 2000).

In this article, we describe a method applicable for SANS in which the neutron scattering length density distribution of an object can be determined directly from the structure factor amplitude, as obtained through the use of a reference attached to each object in a collection of randomly oriented, identical objects in the dilute solution limit (negligible interparticle correlations). The approach presented here is applicable only within the range of validity of the Born approximation. The scattering object is treated as a composite consisting of an 'unknown' part of interest plus a reference component, where the real-space structure of the latter is assumed to be completely known. If, for example, the reference part of the object is composed of a ferromagnetic material (the magnetization of which is saturated), then polarized neutron beams can be employed to extract the information required for an unambiguous inversion of the scattering data without chemical substitution. The angular averaging over all possible relative orientations of the composite object does not result in

a cancellation of the phase information since the reference and unknown segment of each object have a fixed spatial relationship [unlike molecular-scale holographic techniques which require orientational order (Sur *et al.*, 2001)].

The new method proposed here is not simply another type of isomorphic substitution, but also involves a reformulation of the underlying mathematical analysis of this particular scattering problem. Instead of extracting a radius of gyration or distance distribution function (see *e.g.* Glatter & Kratky, 1982), a finite element approach in conjunction with a rearrangement of the structure factor expressions, including the angular averaging over all possible orientations of the sample object, allows for a direct and unambiguous determination of the SLD distribution. Alternatively, more modern methods of small-angle scattering analysis (see *e.g.* Svergun & Koch, 2003) may be, to some extent, applicable to the phase-sensitive technique presented here.

In principle, the method proposed in this article should be applicable to macromolecules, in solution, ranging in size from dimensions of tens to hundreds of ångström. One area of particular interest would be protein molecules that cannot be crystallized for conventional X-ray diffraction studies.

2. Theoretical basis

Consider a composite object consisting of a component of interest, which has a shape and a distribution of scattering length density $\rho(\mathbf{r})$ that are unknown, and an adjacent (and attached) reference part which is completely characterized, as depicted schematically in Fig. 1. For clarity of exposition, it is assumed (without loss of generality) that the reference part is a simple rectangular solid of uniform SLD and centered on the origin of the reference frame fixed to the sample object. The rectangular reference has edges parallel to the x, y and z axes. The other component, which can be of any shape and SLD distribution, is divided into sub-units of equal cubic volume which can be made as small as commensurate with the length scale being probed in a scattering measurement (as determined by the maximum value of the scattering vector $\mathbf{Q}$ attainable). The SLD distribution of the unknown part is thereby described to the requisite degree of accuracy by a properly ordered array of finite elements, an approach commonly taken in both reflectometry (see *e.g.* Majkrzak *et al.*, 2003) and SANS (Barnes & Zemb, 1988) (for a general reference to SANS methods, see *e.g.* Glatter & Kratky, 1982; Feigin & Svergun, 1987; Svergun & Koch, 2003; Hammouda, 2013). (We assume that the SLDs of all components are purely real, as is commonly the case for neutron scattering from materials where absorption is negligible.)

Once again, we assume a collection of randomly oriented, identical objects in the dilute solution limit (negligible interparticle correlations). The structure factor for any one of the identical objects in the ensemble, averaged over all possible angular orientations, is proportional to a differential scattering cross section. For the purposes of this discussion, we can neglect sample volume normalization factors and set the SLD of the solution to be zero. Prior to orientational averaging, the structure factor, F_C, as defined within the Born approximation, for a single composite object is given by

$$F_C(\mathbf{Q}) = \iiint_{zyx} \rho(\mathbf{r}) \exp(i\mathbf{Q}\cdot\mathbf{r})\,\mathrm{d}\mathbf{r} = \iiint_{zyx} \rho(x,y,z) \exp[i(Q_x x + Q_y y + Q_z z)]\,\mathrm{d}x\,\mathrm{d}y\,\mathrm{d}z, \quad (1)$$

where the integration is over the entire volume of the object (both unknown and reference parts) and the scattering vector $\mathbf{Q}$ and the position vector $\mathbf{r}$ are expressed in the object coordinate system (x, y, z). We can write the composite structure factor F_C as the sum of two parts, one for the unknown part of the object and the other for the reference piece (this corresponds to the sum of two integrals, each performed over the respective partial volume):

$$F_C(\mathbf{Q}) = F_R(\mathbf{Q}) + F_S(\mathbf{Q}), \quad (2)$$

where the subscripts R and S denote the reference and unknown 'sample of interest' parts of the composite object. In any scattering experiment, a reflected intensity is measured, which is proportional to the complex square of the structure factor. For a symmetric component F_R, this is given by

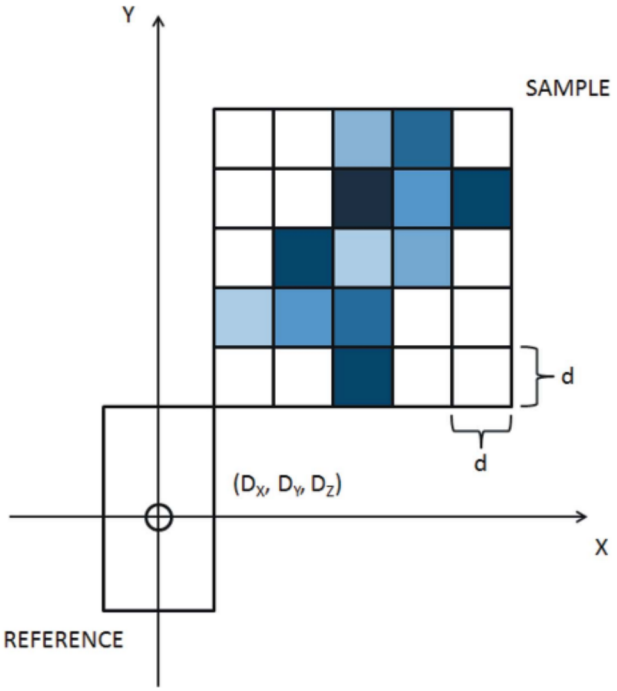

Figure 1
Diagram of a composite object (only a two-dimensional cut perpendicular to the z axis is shown) consisting of some arbitrary component of interest, which has a shape and a distribution of scattering length density that are unknown, and an adjacent (and attached) reference part, which is completely characterized. For clarity of exposition, it is assumed, without loss of generality, that the reference part is a simple rectangular solid of uniform SLD and centered on the origin of the reference frame fixed to the composite object. Thus, the reference part of the composite object is symmetric in this coordinate system. (The dimensions of the reference part are $2D_x \times 2D_y \times 2D_z$.) The other component, which can be of any shape and SLD distribution, is divided into sub-units of equal cubic volume d^3. This coordinate system is fixed with respect to the object.

$$|F_C|^2 = |F_R|^2 + |F_S|^2 + 2\mathrm{Re}F_R\mathrm{Re}F_S, \quad (3)$$

since F_R is real for a symmetric reference.

For the problem at hand, the expression in (3) must be averaged over the entire solid angle. Thus, denoting this orientational average by $\langle\rangle$, we need

$$\langle|F_C|^2\rangle = \langle|F_R|^2\rangle + \langle|F_S|^2\rangle + \langle 2\mathrm{Re}F_R\mathrm{Re}F_S\rangle. \quad (4)$$

Practical matters aside, it is conceptually useful to realize that the R and S parts of C actually need not be 'physically' attached to each other. It is required only that they behave so with regard to mutual orientations. In other words, the composite object C can be considered to consist of the two parts R and S rigidly joined by an imaginary rod. One can therefore view the 'interparticle' interference between R and S as the source of the phase information needed to extract the structure of S. However, the rotational symmetry of S relative to R is important; for example, if R is isotropic, then only the isotropic or rotationally averaged part of S can be determined.

Now suppose that, in principle at least, the reference part of the composite object could be replaced with a piece of identical size and shape but with a different uniform SLD (how this could be accomplished in practice is discussed later on). Two independent scattering experiments could then be performed, one for an ensemble of composite objects with reference part 'A' and the other with reference part 'B', the sample part of each object being the same (F_R for either A or B could also be zero). The difference between the two data sets of reflected intensities thus collected is proportional to the difference in the corresponding orientationally averaged square of the composite structure factors. Defining this difference function to be $D(Q)$, the following relation can be written using equation (4):

$$D(Q) \equiv \langle|F_{CA}|^2\rangle - \langle|F_{CB}|^2\rangle = \langle|F_{RA}|^2\rangle - \langle|F_{RB}|^2\rangle + 2U(Q), \quad (5)$$

where

$$U(Q) = \langle\mathrm{Re}F_{RA}\mathrm{Re}F_S\rangle - \langle\mathrm{Re}F_{RB}\mathrm{Re}F_S\rangle \quad (6)$$

and the subscripts RA and RB refer to the two different reference parts successively attached to the common sample part of the composite scattering object. Since $U(Q)$ can be measured while $\langle|F_{RA}|^2\rangle$ and $\langle|F_{RB}|^2\rangle$ can be computed, then $U(Q)$ is a quantity that can be directly solved for: *i.e.*

$$\begin{aligned} U(Q) &= \tfrac{1}{2}[{}_{\mathrm{MEAS}}D(Q) - ({}_{\mathrm{CALC}}\langle|F_{RA}|^2\rangle - {}_{\mathrm{CALC}}\langle|F_{RB}|^2\rangle)] \\ &= (\langle\mathrm{Re}F_{RA}\mathrm{Re}F_S\rangle - \langle\mathrm{Re}F_{RB}\mathrm{Re}F_S\rangle), \end{aligned} \quad (7)$$

which is an implicit equation for the desired $\mathrm{Re}F_S$ that is embedded within the orientational average as a product with the real part of the known quantities $\mathrm{Re}F_{RB}$ and $\mathrm{Re}F_{RA}$. In the special case where $\mathrm{Re}F_S$ is isotropic, it can be taken out of the orientational average and directly solved for. For the general – and more interesting – case, however, we cannot so easily extract $\mathrm{Re}F_S$ from the average in which it is embedded. On the other hand, $\mathrm{Re}F_S$ itself is not what we are ultimately looking for but, rather, the function $\rho_S(\mathbf{r})$, of which F_S is the Fourier transform. We now show, with the aid of a piecewise continuous representation of $\rho_S(\mathbf{r})$ over a suitable three-dimensional mesh of cubical cells, that a set of discrete element values defining $\rho_S(\mathbf{r})$ to the desired accuracy can indeed be extracted from the right-hand side of equation (7) through an algebraic rearrangement of terms and subsequent solution of a set of linear simultaneous equations. We begin by writing explicit expressions for the structure factors F_R and F_S.

The structure factor for the rectangular solid reference part of the object, F_R, centered on the composite object coordinate system, is given by

$$\begin{aligned} F_R &= \iiint_{zyx} \rho_R \exp(i\mathbf{Q}\cdot\mathbf{r})\,\mathrm{d}\mathbf{r} \\ &= \iiint_{zyx} \rho_R \exp[i(Q_x x + Q_y y + Q_z z)]\,\mathrm{d}x\,\mathrm{d}y\,\mathrm{d}z \\ &= \rho_R \iiint_{zyx} \exp(iQ_x x)\exp(iQ_y y)\exp(iQ_z z)\,\mathrm{d}x\,\mathrm{d}y\,\mathrm{d}z \\ &= [8\rho_R/(Q_xQ_yQ_z)]\sin(Q_xD_x)\sin(Q_yD_y)\sin(Q_zD_z) \\ &= \mathrm{Re}F_R, \end{aligned} \quad (8)$$

where the integration limits are from $-D_x$ to $+D_x$ and similarly in the other two directions. In the above expression, the dimensions of the rectangular reference are $2D_x$, $2D_y$ and $2D_z$ as indicated in Fig. 1. The uniform SLD of the reference, ρ_R, has units of inverse length squared.

The structure factor for the sample part of the object has a more complicated form, one which can describe an arbitrary shape and SLD distribution, and is given by (where the integration limits are now from D_x to $D_x + Ld$ and analogously along the **y** and **z** directions)

$$F_S = \iiint_{zyx} \rho_S(x,y,z)\exp(iQ_x x)\exp(iQ_y y)\exp(iQ_z z)\,\mathrm{d}x\,\mathrm{d}y\,\mathrm{d}z. \quad (9)$$

Consider, for example, an expansion of the integration along the **x** direction in equation (9):

$$\begin{aligned} \int_x \rho_S(x,y,z)\exp(iQ_x x)\,\mathrm{d}x &= \rho_{S1}(y,z)\int_{D_x}^{D_x+d}\exp(iQ_x x)\,\mathrm{d}x \\ &\quad + \rho_{S2}(y,z)\int_{D_x+d}^{D_x+2d}\exp(iQ_x x)\,\mathrm{d}x + \cdots \\ &\quad + \rho_{Sl}(y,z)\int_{D_x+(l-1)d}^{D_x+ld}\exp(iQ_x x)\,\mathrm{d}x \\ &\quad + \rho_{SL}(y,z)\int_{D_x+(L-1)d}^{D_x+Ld}\exp(iQ_x x)\,\mathrm{d}x \\ &= \sum_{l=1}^{L}\rho_{Sl}(y,z)(2/Q_x)\exp\{iQ_x[D_x \\ &\quad + (d/2)(2l-1)]\}\sin(Q_x d/2). \end{aligned} \quad (10)$$

After doing similarly along the **y** and **z** directions, we obtain

$$\begin{aligned} \mathrm{Re}F_S &= [8/(Q_xQ_yQ_z)]\sin(Q_xd/2)\sin(Q_yd/2)\sin(Q_zd/2) \\ &\quad \times \sum_{l=1}^{L}\sum_{m=1}^{M}\sum_{n=1}^{N} {}_S\rho_{lmn}\cos\{Q_x[D_x - (d/2) + ld] \\ &\quad + Q_y[D_y - (d/2) + md] + Q_z[D_z - (d/2) + nd]\}, \end{aligned} \quad (11)$$

where d is the edge of a sub-unit cube of the sample part of the object's volume, which is rendered into $L \times M \times N$ such sub-units, each one having an individual but constant SLD, ${}_{\rm S}\rho_{lmn}$, corresponding to the (l, m, n)th sub-unit.

Using equations (7), (8) and (11), we can now write the function $U(Q)$ explicitly as

$$\begin{aligned} U(Q) &= \langle {\rm Re}F_{\rm RA}{\rm Re}F_{\rm S}\rangle - \langle {\rm Re}F_{\rm RB}{\rm Re}F_{\rm S}\rangle \\ &= \langle {\rm Re}F_{\rm RA}{\rm Re}F_{\rm S} - {\rm Re}F_{\rm RB}{\rm Re}F_{\rm S}\rangle \\ &= \langle ({\rm Re}F_{\rm RA} - {\rm Re}F_{\rm RB}){\rm Re}F_{\rm S}\rangle \\ &= \langle [8/(Q_xQ_yQ_z)]^2(\rho_{\rm RA} - \rho_{\rm RB}) \\ &\quad \times \sin(Q_xD_x)\sin(Q_yD_y)\sin(Q_zD_z) \\ &\quad \times \sin(Q_xd/2)\sin(Q_yd/2)\sin(Q_zd/2) \\ &\quad \times \sum_{l=1}^{L}\sum_{m=1}^{M}\sum_{n=1}^{N} {}_{\rm S}\rho_{lmn}\cos\{Q_x[D_x - (d/2) + ld] \\ &\quad + Q_y[D_y - (d/2) + md] + Q_z[D_z - (d/2) + nd]\}\rangle \quad (12) \end{aligned}$$

or

$$U(Q) = \sum_{l=1}^{L}\sum_{m=1}^{M}\sum_{n=1}^{N} {}_{\rm S}\rho_{lmn}\langle C_{lmn}(Q_x, Q_y, Q_z)\rangle. \quad (13)$$

Equation (12) represents a system of linear equations for LMN unknowns ${}_{\rm S}\rho_{lmn}$ with coefficients that can be calculated on the right-hand side and values of the function $U(Q)$ on the left-hand side which can be determined from two independent scattering measurements, as discussed previously. A numerical solution of equation (12) is given in §4 for a model structure, as an illustrative example.

The angular averaging of the coefficients in equation (12) is performed over all possible orientations of the object relative to the scattering vector **Q** fixed in the laboratory frame of reference. To do this, we describe **Q** in the object reference frame where its rectangular components can be expressed in terms of the Euler angles (Goldstein, 1980).

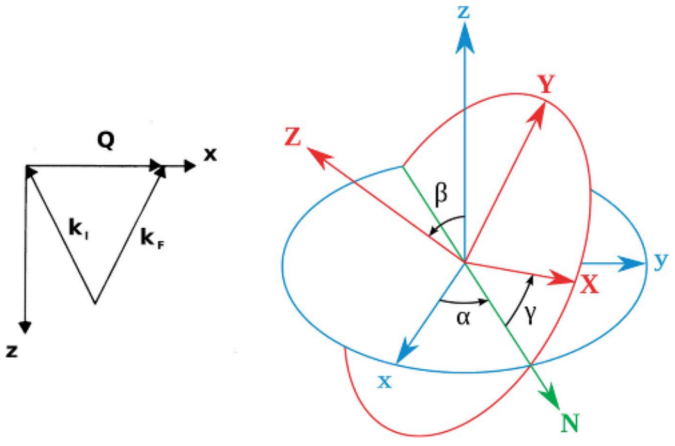

Figure 2
The schematic (on the right) illustrates the relationship between the axes of the object and laboratory in terms of the Euler angles (Goldstein, 1980). The diagram on the left shows the scattering geometry in the laboratory frame of reference for one plane of a continuum rotated about the incident beam direction (along the nominal $\mathbf{k}_I$ direction). ($\mathbf{Q} = \mathbf{k}_F - \mathbf{k}_I$.) (Right part of figure courtesy of L. Brits, *Wikipedia*.)

The (l, m, n)th coefficient, C_{lmn}, is given by

$$\begin{aligned} \langle C_{lmn}(Q_x, Q_y, Q_z)\rangle &= \langle [8/(Q_xQ_yQ_z)]^2(\rho_{\rm RA} - \rho_{\rm RB})\sin(Q_xD_x) \\ &\quad \times \sin(Q_yD_y)\sin(Q_zD_z)\sin(Q_xd/2)\sin(Q_yd/2) \\ &\quad \times \sin(Q_zd/2)\cos\{Q_x[D_x - (d/2) + ld] \\ &\quad + Q_y[D_y - (d/2) + md] + Q_z[D_z - (d/2) + nd]\}\rangle. \quad (14) \end{aligned}$$

Here the orientational averaging is defined (Andrews, 2004) as

$$\langle C_{lmn}(Q_x, Q_y, Q_z)\rangle = \frac{1}{8\pi^2}\int\!\!\int\!\!\int_{\alpha\beta\gamma} C_{lmn}(\alpha, \beta, \gamma)\sin\beta\,{\rm d}\beta\,{\rm d}\alpha\,{\rm d}\gamma, \quad (15)$$

in which the integration limits for the angles α, β and γ are zero to 2π, π and 2π, respectively, and the rectangular components of **Q**, (Q_x, Q_y, Q_z), in the object coordinate system are expressed in terms of the angles of integration by

$$\begin{aligned} Q_x &= Q(\cos\gamma\cos\alpha - \cos\beta\sin\alpha\sin\gamma), \\ Q_y &= Q(-\sin\gamma\cos\alpha - \cos\beta\sin\alpha\cos\gamma), \\ Q_z &= Q(\sin\beta\sin\alpha), \\ Q &= |\mathbf{Q}| = (Q_x^2 + Q_y^2 + Q_z^2)^{1/2} = [4\pi\sin({\rm SA}/2)]/\lambda. \end{aligned} \quad (16)$$

Here SA is the scattering angle between $\mathbf{k}_I$ and $\mathbf{k}_F$ (**Q** has been taken to be directed along the X axis of the laboratory coordinate system). Fig. 2 is a schematic illustrating the relationship between the axes of the object and laboratory through the Euler angles (Goldstein, 1980).

In principle, the phase-sensitive method developed in this section for SANS within the Born approximation is applicable to small-angle X-ray scattering as well, but with some modification necessary to account for nonnegligible absorption. When absorption is nonnegligible, the SLD is a complex quantity where the imaginary component is associated with the absorption process as opposed to the real part which gives rise to coherent scattering. If the SLD has both real and imaginary parts, then additional measurements with more than two references are required to obtain the SLD distribution for the object sample part of interest.

3. Practical references

3.1. Ferromagnetic materials

One possible reference choice for SANS, if a polarized incident beam and polarization analysis of the reflected beam is available, is a ferromagnetic material, saturated in a remanent state either along a specific direction in the reference frame fixed to each object or along a single direction in the laboratory frame of reference as defined by the application of an external magnetic field. Recent polarized SANS work has focused on magnetic particle structure determination (Krycka *et al.*, 2013; Disch *et al.*, 2012). For a nonmagnetic sample part of the object, the selection rules for polarized neutron scattering (Moon *et al.*, 1969) are such that only non-spin-flip scattering processes convey structural information. If neutrons are incident in the '+' state (one of two possible spin eigen-

states), then the reflected beam will also be in that same polarization state, and analogously for an incident beam in the '−' state. Taking the neutron polarization axis to be along the **Z** direction in the laboratory frame of reference, the two corresponding expressions for the SLDs for a polarized neutron beam are given by

$$\rho = \rho_{\rm N} \pm \rho_{\rm M} q_{HVZ}, \tag{17}$$

where $\rho_{\rm N}$ and $\rho_{\rm M}$ correspond to the nuclear and magnetic SLDs, respectively, $\pm$ indicates the neutron spin state, and q_{HVZ} is the Z component of the Halperin vector (Moon *et al.*, 1969), which determines the extent of the coupling between the neutron spin and the atomic magnetic moments of the material through the relationship

$$q_{HVZ} = \cos\varphi_{QZ}\cos\varphi_{QS} - \cos\varphi_{SZ}. \tag{18}$$

Here φ_{QZ} is the angle between **Q** and the neutron polarization direction (already specified to be the laboratory Z axis), φ_{QS} is the angle between **Q** and the atomic spin (opposite to its associated magnetic moment), and φ_{SZ} is the angle between the atomic spin and the laboratory Z axis.

For the specific case where the neutron polarization **P** is along the laboratory Z axis (which is perpendicular to **Q**, which in turn has been taken to lie along the laboratory X axis) and each object's ferromagnetic magnetization points along the laboratory Z axis as well (by application of an applied external magnetic field), then $q_{HVZ} = +1$ so that

$$\rho = \rho_{\rm N} \pm \rho_{\rm M}. \tag{19}$$

The nuclear and magnetic contributions to the overall SLD of the reference part effectively add or subtract depending on the spin state of the incident neutron. (In practice, it is simpler to maintain the neutron polarization axis along the incident beam direction $\mathbf{k}_{\rm I}$, but the correction for this case is small compared to that for which **P** is always arranged to be exactly perpendicular to **Q** and the difference has negligible consequences for the simpler example we have chosen to illustrate.) Two references are thereby achieved without any physical change to the composite object, and all that is required is to collect two scattered intensity data sets, one for neutron spin plus and the other for spin minus incident, to obtain $U(Q)$. Note that in this particular case, the magnetic reference in conjunction with polarized neutron beam measurements is essentially equivalent to an isotopic exchange of material with a different nuclear SLD in the reference part.

Alternatively, if the neutron polarization **P** is still along the laboratory Z axis (again, perpendicular to **Q** which is along the laboratory X axis) but the magnetization of each object is always directed along the negative z axis of the coordinate system fixed in the same orientation to each object (in a remanent state), then ρ is given by

$$\rho = \rho_{\rm N} \pm \rho_{\rm M}\cos\beta, \tag{20}$$

where $\cos\beta$ is simply the direction cosine between a given object's z axis and the Z axis of the laboratory reference system.

In both of the relatively simple configurations presented above, the assumption of a randomly oriented collection of objects within the total sample volume, along with the choice of polarization axis to be orthogonal to **Q**, ensures angular isotropy about the laboratory Z axis perpendicular to **Q**. However, this particular choice of symmetry is not required, and the neutron polarization axis may be selected to lie along another direction in the laboratory frame of reference, if it is advantageous to do so for other reasons.

3.2. Composite structure: nonmagnetic reference part plus 'unknown' part

Although the use of polarized neutrons and saturated ferromagnetic references attached to the sample of interest may have certain distinct advantages, there are other reference possibilities. Suppose, for instance, that the sample object of interest can be chemically attached to a known molecular structure.

Then, in analogy to equation (4) we can write

$$\langle|F_{\rm C}|^2\rangle = \langle|F_{\rm KR}|^2\rangle + \langle|F_{\rm TBD}|^2\rangle + \langle 2{\rm Re}F_{\rm KR}{\rm Re}F_{\rm TBD}\rangle, \tag{21}$$

where it is assumed that the scattered intensity as a function of **Q** can be measured in separate experiments for (1) the composite system (denoted by the subscript C); (2) the 'known reference' part KR alone (taken to be symmetric and not yet attached to the unknown 'to be determined' part TBD); and (3) the unknown part TBD by itself. Since all of the components on the right-hand side of equation (21) can be measured independently ($\langle|F_{\rm KR}|^2\rangle$ could also be calculated, in principle) and ${\rm Re}F_{\rm KR}$ can be calculated, then the SLDs associated with a finite element decomposition of TBD, the part of interest, can be determined in the same way as shown previously in the derivation culminating in equation (12).

As long as the structure factor for the composite object can be expressed as a sum of separable terms, one for the sample part and the other corresponding to the reference component, then the method presented here is applicable. For example, it is possible to adopt a configuration in which the reference volume is contained within that of the sample component or *vice versa*, assuming that the structure and material composition of the reference part is completely known in either case.

The choice of reference is not completely arbitrary, however. The symmetry of the reference part can be important. For example, consider a simple two-dimensional square sample object divided into four square sub-cells, where the reference part is also taken to be square ($D_x = D_y$) with its sides parallel to those of the sample part of the composite object. Then the inversion of $U(Q)$ can only yield SLD values for the two sample sub-cells lying along a diagonal perpendicular to the reference diagonal that runs from the origin out to the point (D_x, D_y) which are equal to their average. Optimization of the reference structure can be an important consideration.

Table 1
Original model SLDs and the corresponding set obtained by inversion of $U(Q)$ as described in the text.

Sub-cell index	Model SLD (Å^{-2})	SLD *via* inversion of $U(Q)$ (Å^{-2})
1	8.0×10^{-6}	$7.9952567492373344 \times 10^{-6}$
2	5.0×10^{-6}	$5.1581725329032674 \times 10^{-6}$
3	3.0×10^{-6}	$3.0569598364690891 \times 10^{-6}$
4	0.0	$-7.2533473459990216 \times 10^{-8}$
5	0.0	$-1.5660148421135301 \times 10^{-7}$
6	2.0×10^{-6}	$2.2978778672140286 \times 10^{-6}$
7	5.0×10^{-6}	$4.8739136996700097 \times 10^{-6}$
8	3.0×10^{-6}	$2.9930326061456065 \times 10^{-6}$
9	2.0×10^{-6}	$2.1984348123739998 \times 10^{-6}$
10	3.0×10^{-6}	$2.9629299578242556 \times 10^{-6}$
11	2.0×10^{-6}	$2.1925726598984072 \times 10^{-6}$
12	2.0×10^{-6}	$1.6436400553807519 \times 10^{-6}$
13	5.0×10^{-6}	$4.7519473764813062 \times 10^{-6}$
14	0.0	$1.5486577358675494 \times 10^{-7}$
15	3.0×10^{-6}	$3.1727620721836486 \times 10^{-6}$
16	8.0×10^{-6}	$7.9598602881746376 \times 10^{-6}$
17	0.0	$-6.9083620588432130 \times 10^{-7}$
18	5.0×10^{-6}	$5.2662142595539992 \times 10^{-6}$
19	2.0×10^{-6}	$2.2331881840833366 \times 10^{-6}$
20	3.0×10^{-6}	$2.7336203622214004 \times 10^{-6}$
21	5.0×10^{-6}	$4.9615602336763678 \times 10^{-6}$
22	2.0×10^{-6}	$2.2545626421854936 \times 10^{-6}$
23	0.0	$2.2333899747162826 \times 10^{-7}$
24	0.0	$-5.4189888528353584 \times 10^{-8}$
25	3.0×10^{-6}	$2.8814918203719384 \times 10^{-6}$
26	5.0×10^{-6}	$5.0080273594332235 \times 10^{-6}$
27	8.0×10^{-6}	$7.9999309055434301 \times 10^{-6}$

4. Illustrative example

Fig. 3 is an exploded view of a model SLD distribution described within a volume containing 27 cubic sub-cells, each 10 Å on a side. Adjacent to this sample object, a ferromagnetic reference consisting of a rectangular block of dimensions (2 × 15 Å) × (2 × 25 Å) × (2 × 35 Å) along the x, y and z axes, respectively, is centered at the origin of the composite object reference system. The ferromagnetic material of the reference is taken to be saturated by an applied magnetic field along the Z axis of the laboratory reference frame, perpendicular to **Q**. Using a polarized neutron incident beam and polarization analysis of the scattered beam, as described in the previous section, two values of the reference SLD can be obtained without any chemical change to the composite scattering object. The two SLD values are $\rho = \rho_N \pm \rho_M$. (The SLD value of each of the sample object's sub-cells is given in Table 1.) The scattering function $U(Q)$ as calculated from the formulas derived in earlier sections using the model values of the sub-cell SLDs is plotted in Fig. 4.

The set of simultaneous equations represented by (12) (after computing the requisite coefficients averaged over angular orientation) were solved numerically by singular value decomposition (SVD) (Press *et al.*, 1992) for the distribution of SLD values of the sample sub-cells assuming a set of $U(Q)$ values generated for the original model SLD values. Both the original model SLDs and the corresponding set obtained by inversion of $U(Q)$ are listed in Table 1. The same information contained in Table 1 is shown as a histogram in Fig. 5. The agreement between the SLD distribution obtained by inversion of the model-generated scattering function $U(Q)$ and that of the original model is remarkably good. The system of equations was overdetermined with 184 values of $U(Q)$ between 0.001 and 0.323 Å^{-1}. This maximum Q value is just beyond $\pi/10$ Å, which corresponds to the smallest length scale in the object, the side of a sub-cell, and is the range required to obtain that spatial resolution. The relatively small but finite discrepancies between model SLDs and the values obtained *via* the inversion are presumed to be associated with the accuracy of the limited numerical methods employed; further

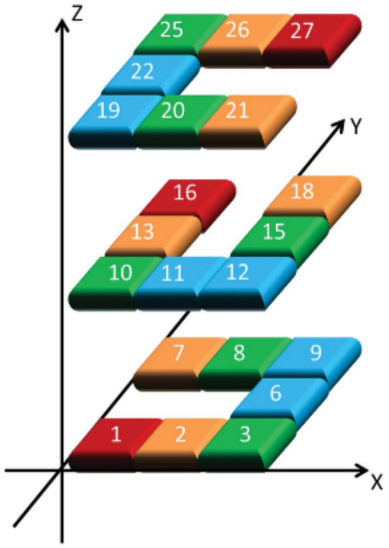

Figure 3
An exploded view (the layers are actually in contact with one another along the z axis) of a model SLD distribution described within a volume containing 27 cubic sub-cells, each 10 Å on a side. Adjacent to this sample object, a ferromagnetic reference consisting of a single rectangular block of dimensions (2 × 15 Å) × (2 × 25 Å) × (2 × 35 Å), along the x, y and z axes, respectively, is centered at the origin of the composite object reference system and has a uniform SLD. Advancing along the positive z axis, there is a counterclockwise chirality. The alternative index j of the (l, m, n)th sub-cell shown in the diagram is given by $j = (n-1)NM + (m-1)M + l$, where the total number of sub-cells is $L \times M \times N = 3 \times 3 \times 3 = 27$. The SLDs of sub-cells 4, 5, 14, 17, 23 and 24 are zero.

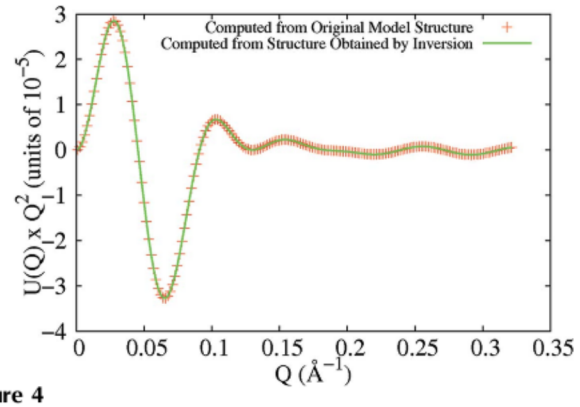

Figure 4
The scattering function $U(Q)$ as calculated from the formulas derived in earlier sections using the model values of the sub-cell SLDs listed in Table 1 multiplied by Q^2 for clarity in the plot (+ symbols). The solid line represents the function $U(Q)$ as calculated for the SLD values obtained by inversion of the original $U(Q)$ computed from the starting model SLD values. The SLD values obtained *via* inversion are also given in Table 1.

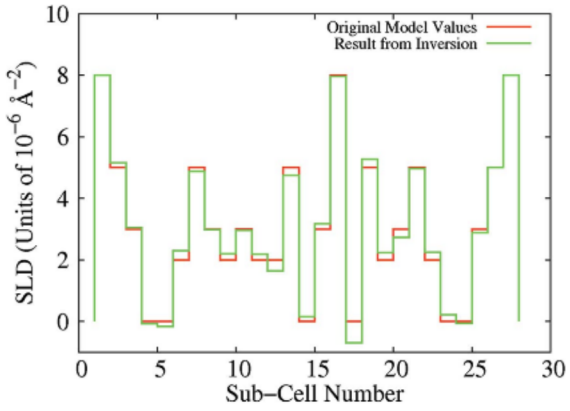

Figure 5
Histogram representation of the distribution of SLD values of the sample sub-cells as solved numerically by singular value decomposition (green line) compared with the original corresponding model values (red line). The same information is contained in Table 1. The agreement between the SLD distribution obtained by inversion of the model-generated scattering function $U(Q)$ and that of the original model is remarkably good.

refinement and optimization may be possible. In Fig. 4, the scattering function $U(Q)$ associated with the original model SLD set of values is also compared with that generated by the SLD values obtained *via* the subsequent inversion.

Using SVD to solve a linear system is regarded to be, numerically, one of the most stable methods. However, a still relatively coarse grid of 20 × 20 × 20 yields 8000 elemental cubes to render the sample object into. To avoid an underdetermined situation, at least the same number of reflected intensity data points must be collected. However, the problem is what it is and there is 'no free lunch': to extract a picture of an object's real density distribution at a given spatial detail requires a commensurate level of information in the diffraction data, as is all too well known. Nonetheless, for the method proposed in this article it is possible, in principle, to at least achieve a unique solution for the structure at a resolution limited only by the range of Q over which reflected intensity is measured and the statistical accuracy of that data. SLD model renderings of the object of interest other than the cubic subcells of uniform density used here, are, of course, possible (see *e.g.* Fedorova & Schmidt, 1978). Alternatively, as mentioned in the *Introduction*, perhaps more modern methods of small-angle scattering analysis (see *e.g.* Svergun & Koch, 2003) may be, to some extent, applicable to the phase-sensitive technique presented here.

5. Conclusions

In this article we have developed a procedure to directly and unambiguously obtain the SLD distribution for a molecular structure *via* SANS through the use of reference structures either physically or chemically attached to the object of interest. The proposed method is applicable for a collection of identical molecular-scale objects which are randomly oriented in angle in solution in the dilute concentration limit (where interparticle correlations are negligible) where the Born approximation is valid. In particular, saturated ferromagnetic references in conjunction with polarized neutron beams make it possible, in principle, to employ a single form of the composite object (*i.e.* without additional chemical substitution) consisting of the component piece of interest and an attached (or embedded) reference, to uniquely determine the SLDs of the finite-element sub-cell structure of the sample piece.

The new method proposed here is not simply another type of isomorphic substitution, but also involves a reformulation of the underlying mathematical analysis of this particular scattering problem. Instead of extracting a radius of gyration or radial distribution function, a finite element approach in conjunction with a rearrangement of the structure factor expressions, including the angular averaging over all possible orientations of the sample object, allows for a direct and unambiguous determination of the SLD distribution. Numerical simulations of the technique presented here on model systems support these conclusions.

Given that the proposed method has been demonstrated in principle here, practical realization will require reference structures that can be used to create the necessary composite samples.

We acknowledge useful and informative discussions with B. Hammouda and T. Jach.

References

Andrews, S. S. (2004). *J. Chem. Educ.* **81**, 877–885.
Barnes, I. S. & Zemb, T. N. (1988). *J. Appl. Cryst.* **21**, 373–379.
Berk, N. F. & Majkrzak, C. F. (1996). *J. Phys. Soc. Jpn*, **65**, 107–112.
Cowley, J. M. (1981). *Diffraction Physics*, 2nd ed. Amsterdam: North Holland.
Disch, S., Wetterskog, E., Hermann, R. P., Wiedenmann, A., Vainio, U., Salazar-Alvarez, G., Bergström, L. & Brückel, T. (2012). *New J. Phys.* **14**, 13025.
Fedorova, I. S. & Schmidt, P. W. (1978). *J. Appl. Cryst.* **11**, 405–411.
Feigin, L. A. & Svergun, D. I. (1987). *Structure Analysis by Small-Angle X-ray and Neutron Scattering*, edited by G. W. Taylor. New York: Plenum Press.
Glatter, O. & Kratky, O. (1982). Editors. *Small Angle X-ray Scattering.* New York: Academic Press.
Goldstein, H. (1980). *Classical Mechanics*, 2nd ed. Reading: Addison-Wesley.
Haan, V. de, van Well, A., Adenwalla, S. & Felcher, G. (1995). *Phys. Rev. B*, **52**, 10831–10833.
Hammouda, H. (2013). *Probing Nanoscale Structures – The SANS Toolbox*, http://www.ncnr.nist.gov/staff/hammouda/the_SANS_toolbox.pdf.
Hauptman, H. (1986). *Science*, **233**, 178–183.
Kasper, J., Leeb, H. & Lipperheide, R. (1998). *Phys. Rev. Lett.* **80**, 2614–2617.
Krycka, K. L., Borchers, J. A., Salazar-Alvarez, G., Lopez-Ortega, A., Estrader, M., Estrade, S., Winkler, E., Zeisler, R. D., Sort, J., Peiro, F., Baro, M. D., Kao, C. C. & Nogues, J. (2013). *ACS Nano*, **7**, 921–931.
Lesslauer, W. & Blasie, J. K. (1971). *Acta Cryst.* A**27**, 456–461.
Majkrzak, C. & Berk, N. (1995). *Phys. Rev. B*, **52**, 10827–10830.
Majkrzak, C. F., Berk, N. F., Ankner, J. F., Satija, S. K. & Russell, T. P. (1992). *Proc. SPIE*, **1738**, 282–304.

Majkrzak, C. F., Berk, N. F. & Perez-Salas, U. A. (2003). *Langmuir*, **19**, 7796–7810.
Moon, R., Riste, T. & Koehler, W. (1969). *Phys. Rev.* **181**, 920–931.
Press, W. H., Teukolsky, S. A., Vetterling, W. T. & Flannery, B. P. (1992). *Numerical Recipes in Fortran: The Art of Scientific Computing*, 2nd ed. New York: Cambridge University Press.
Sanyal, M. K. *et al.* (1993). *Europhys. Lett.* **21**, 691.
Sur, B., Rogge, R. B., Hammond, R. P., Anghel, V. N. & Katsaras, J. (2001). *Nature*, **414**, 525–527.
Svergun, D. I. & Koch, M. H. J. (2003). *Rep. Prog. Phys.* **66**, 1735–1782.
Zimmermann, K., Tolan, M., Weber, R., Stettner, J., Doerr, A. & Press, W. (2000). *Phys. Rev. B*, **62**, 10377–10382.